

# Organized Proteomic Heterogeneity in Colorectal Cancer Liver Metastases and Implications for Therapies

Andrei Turtoi,<sup>1,2</sup> Arnaud Blomme,<sup>1</sup> Delphine Debois,<sup>2</sup> Joan Somja,<sup>3</sup> David Delvaux,<sup>1</sup> Georgios Patsos,<sup>1</sup> Emmanuel Di Valentin,<sup>4</sup> Olivier Peulen,<sup>1</sup> Eugène Nzaramba Mutijima,<sup>3</sup> Edwin De Pauw,<sup>2</sup> Philippe Delvenne,<sup>3</sup> Olivier Detry,<sup>5</sup> and Vincent Castronovo<sup>1</sup>

**Tumor heterogeneity is a major obstacle for developing effective anticancer treatments. Recent studies have pointed to large stochastic genetic heterogeneity within cancer lesions, where no pattern seems to exist that would enable a more structured targeted therapy approach. Because to date no similar information is available at the protein (phenotype) level, we employed matrix assisted laser desorption ionization (MALDI) image-guided proteomics and explored the heterogeneity of extracellular and membrane subproteome in a unique collection of eight fresh human colorectal carcinoma (CRC) liver metastases. Monitoring the spatial distribution of over 1,000 proteins, we found unexpectedly that all liver metastasis lesions displayed a reproducible, zonally delineated pattern of functional and therapeutic biomarker heterogeneity. The peritumoral region featured elevated lipid metabolism and protein synthesis, the rim of the metastasis displayed increased cellular growth, movement, and drug metabolism, whereas the center of the lesion was characterized by elevated carbohydrate metabolism and DNA-repair activity. From the aspect of therapeutic targeting, zonal expression of known and novel biomarkers was evident, reinforcing the need to select several targets in order to achieve optimal coverage of the lesion. Finally, we highlight two novel antigens, LTBP2 and TGFBI, whose expression is a consistent feature of CRC liver metastasis. We demonstrate their *in vivo* antibody-based targeting and highlight their potential usefulness for clinical applications. **Conclusion:** The proteome heterogeneity of human CRC liver metastases has a distinct, organized pattern. This particular hallmark can now be used as part of the strategy for developing rational therapies based on multiple sets of targetable antigens. (HEPATOLOGY 2014;59:924-934)**

See Editorial on Page 757

**D**espite its great promise, clinically used targeted cancer therapy is unfortunately showing only limited success at a very high cost.<sup>1</sup> This failure is partly explained by the high level of genetic heterogeneity of malignant lesions and the fact that carcinogenesis is an evolutionally driven process that recapitulates Darwin's theory of selection of the fittest.<sup>2</sup>

In such an unfavorable context, targeted therapy protocols are reaching only a subpopulation of tumor cells, leading to a punctual increase in the selective pressure, fueling resistance to therapy, and thus failing to cure the patient.<sup>3</sup> The notion of tumor heterogeneity and the apparent random distribution of tumor cells harboring different mutations are supported by recent genetic studies.<sup>4-6</sup> However, the lack of information at the protein level limits the understanding of how genetic

Abbreviations: CRC, colorectal cancer; MALDI, matrix assisted laser desorption ionization; MS, mass spectrometry.

From the <sup>1</sup>Metastasis Research Laboratory, GIGA Cancer, University of Liège, Liège, Belgium; <sup>2</sup>Mass Spectrometry Laboratory, GIGA Research, University of Liège, Liège, Belgium; <sup>3</sup>Laboratory of Experimental Pathology, GIGA Cancer, University of Liège, Liège, Belgium; <sup>4</sup>GIGA-Viral Vectors Platform, University of Liège, Liège, Belgium; <sup>5</sup>Dept. of Abdominal Surgery and Transplantation, University Hospital Liège, Liège, Belgium.

Received February 4, 2013; accepted June 20, 2013.

Supported by grants from the University of Liège (Concerted Research Action Program IDEA project), EU (FP7 network: ADAMANT) Wallonian Region Fund (BIOWIN RADIODTARGET project), and from the National Fund for Scientific Research (FNRS). A.T. and D.D. are FNRS research fellows. A.B. is Télévie-FNRS Ph.D. fellow. This work was published with the support of the Belgian University Foundation.

heterogeneity translates into phenotype. Because evolution selects phenotype, interrogating proteins in the context of tumor heterogeneity will certainly prove extremely useful in the clinic. Driven by this concept and the above findings, we have devised a proteomic approach to explore intratumoral heterogeneity in human colorectal cancer (CRC) liver metastasis. CRC is particularly relevant as it is the second leading cause of cancer mortality worldwide,<sup>7</sup> mainly due to the development of liver metastases, which today lack efficient treatments.<sup>8,9</sup> We collected a unique series of well-characterized, freshly sampled, CRC liver metastases (33 patients) and performed unbiased matrix assisted laser desorption ionization (MALDI)-mass spectrometry (MS)-based imaging<sup>10-12</sup> (14 cases) followed by in-depth proteomic analysis (8 patients). The analysis led to an intriguing observation of a reproducible, zone-like, differential distribution of peptides within metastatic lesions. The delineated zones were subsequently macroscopically dissected and subjected to enrichment and quantitative proteomic analysis of membrane and extracellular proteins (further referred to as potentially “accessible”). These proteins have a high likelihood of being reached by way of systemically injected compounds (e.g., antibodies), and as such they represent the most valuable entity for therapeutic targeting and medical imaging applications. Our results demonstrate for the first time that proteome heterogeneity of CRC liver metastases follows a different, more organized pattern than could ever be inferred from existing genetic studies. We highlight two novel protein targets in the context of liver metastases, LTBP2 and TGFBI, which are ubiquitously expressed in a large collection of liver metastases and are absent in normal human tissues (including inflammatory liver diseases), and demonstrate their *in vivo* targeting in an animal model of human CRC. Collectively, these findings represent a new basis for the development of effective, more structured targeted-therapy approaches aimed to improve the outcome of cancer patients.

## Patients and Methods

**Patients and Material.** Human subjects involved in the current study had undergone surgery for

removal of liver metastases caused by disseminating CRC. They were informed about the objectives of the study and gave their written consent. Further information regarding the medical details of individual patients are outlined in Supporting Table S3. First, 14 patients were chosen for MALDI-imaging/proteomic analysis. When fresh material was available and of sufficient size both MALDI-imaging and proteomic analysis were conducted (patients 1-8), otherwise only MALDI-imaging was performed. The Ethical Committee of the University Liege, Belgium approved the study.

**MALDI-MS Imaging.** Paraffin-embedded CRC liver metastases from 14 patients (patient 1-14, detailed in Supporting Table S3) and three primary CRC (matched tissues from patients 9, 11 and 14) were cut at 10  $\mu\text{m}$  thickness and deposited on ITO-coated slides (Bruker, Bremen, Germany). These were deparaffinized and subjected to antigen-retrieval as described for the immunohistochemistry application below. Subsequently, the tissue sections were covered with 1 mL of 50 mM ammonium-bicarbonate, trypsin-containing solution (sequencing grade [Promega, Fitchburg, WI, USA]; 0.05  $\mu\text{g}/\text{mL}$ ). The slides were incubated at room temperature (RT) for 2 minutes with the solution on top. Next, the solution was removed, the slides were air-dried at RT for 1 minute, and incubated in the cell culture incubator (37°C, 95% humidity and 5% CO<sub>2</sub>) for 4 hours. Following this, the slides were dried at 60°C for 30 minutes and subjected to MALDI matrix coating (ImagePrep, Bruker) with alpha-cyano-4-hydroxycinnamic acid (5 mg/mL dissolved in 70  $\mu\text{L}$  acetonitrile and 30  $\mu\text{L}$  trifluoroacetic acid (0.2  $\mu\text{L}$ ) water-solution [Sigma]). Coated slides were imaged using an Ultraflex II MALDI-MS instrument (Bruker). MS spectra were collected in automated mode (300 shots/pixel; 150 pixel/image) and calibrated according to peptide standard (Part-No. #222570; Bruker) which was deposited next to the sample. The images were evaluated using the FlexImaging software (version 3.0; Bruker).

**Sample Preparation and Isolation of Accessible Proteins.** Fresh liver metastases from eight individual patients were used for the proteomic analysis (patients

---

Address reprint requests to: Vincent Castronovo, M.D., Ph.D., or Andrei Turtoi, Ph.D., Metastasis Research Laboratory, GIGA Cancer, University of Liège, 4000 Liège, Belgium. E-mail: vcastronovo@ulg.ac.be, a.turtoi@ulg.ac.be

Copyright © 2014 by the American Association for the Study of Liver Diseases.

View this article online at [wileyonlinelibrary.com](http://wileyonlinelibrary.com).

DOI 10.1002/hep.26608

Potential conflict of interest: Nothing to report.

Additional Supporting Information may be found in the online version of this article.

1-8, Supporting Table S3). The tissue was macroscopically fully dissected in multiple pieces (25 mm<sup>2</sup>). Three quarters of the sample were used for subsequent proteomic analysis, whereas one-quarter was snap-frozen and kept for western blot validation. Further details are provided in the Supporting Materials.

**Quantitative Proteomic Analysis.** Five micrograms of digested protein samples were purified using C18-ZipTip (Millipore, Billerica, MA), desiccated and dissolved in 100 mM ammonium-formiate buffer containing IS3 (MassPREP Digestion Standard Mixture 1 [Waters, Milford, MA] adjusted to 135 fmol/10  $\mu$ L with respect to yeast alcohol dehydrogenase). Half of each of the prepared samples was injected on the nano-UPLC-qTOF MS system comprised of nanoAcquity high-performance liquid chromatography (HPLC; Waters) coupled with the SYNAPT G1 mass spectrometer (Waters, Manchester, UK). The analysis was further performed as described previously.<sup>13,14</sup>

**Principal Component Analysis, Pearson Correlation Clustering, and Functional Evaluation.** Individual proteins and their corresponding absolute protein quantities were uploaded in the Multi Experiment Viewer software v. 4.8<sup>15</sup> and subjected to unsupervised principal component analysis (PCA) and to Pearson correlation clustering. Clusters of expression were identified and color-coded according to the different intratumoral localization. Individual clusters were then exported along with their expression values and were further analyzed with Ingenuity Pathways Analysis software (Ingenuity Systems, Redwood City, CA). The proteins were interrogated for their molecular functions and assessed for networking.

**Immunohistochemical Analysis.** Immunohistochemistry (IHC) analysis of five novel antigens was conducted as experimentally detailed in the Supporting Materials. Nineteen individual CRC-LM cases were involved in the IHC analysis.

**Verification of Protein Modulation Using Western Blot (WB) Analysis.** Of the modulated protein identified in the proteomic analysis, TGFBI and LTBP2 were further selected and verified using WB analysis in eleven additional CRC liver metastasis patients. Further details are provided in the Supporting Materials.

## Results

**CRC Liver Metastases Display a Zonal Pattern of Peptide/Protein Heterogeneity.** Trans-tumor sections of 14 CRC liver metastases were subjected to peptide MALDI-imaging (Fig. 1A-E). The resulting, most intense (signal  $\geq 4 \times 10^2$  counts/sec), peptide ions

from individual MS spectra were verified for their intrametastatic distribution. The analysis identified sets of peptides that displayed reproducible regional presence/absence in liver metastases, subdividing the lesions in three main zones: (1) *peritumoral* (e.g., ions 1515.9 m/z and 1128.6 m/z), consisting of normal liver tissue bordering the metastasis; (2) *rim* (e.g., 2484.7 m/z and 2006.2 m/z); and (3) *center* (e.g., 1105.6 m/z and 3369.3 m/z). Average MALDI-MS spectra corresponding to each individual zone are shown in Supporting Fig. S1a-d. From a histological point of view, the peritumoral zone consisted of hepatocytes and was histologically identical with the normal liver tissue (data not shown). The rim of the metastasis was composed of tumoral cells embedded in desmoplastic reaction (Fig. 1C). The center of the metastasis featured similar cellular composition as the rim region (Fig. 1C); however, the desmoplastic reaction was more prominent and occasionally (especially in larger lesions e.g., >3 cm in diameter) isolated groups of necrotic cells were also observable. The zonal distribution was also present in all CRC liver metastases studied (Fig. 1D) and present in CRC of matched primary tumors of three individuals (Fig. 1E).

We further hypothesized that the zonal pattern of protein expression is probably enforced by microenvironmental factors. The most probable one is the vascularization of the metastatic lesion. Changes in blood supply bring along variations in oxygenation and nutrient availability, which are potent factors that can promptly impact protein expression. To evaluate this possibility we stained tissue sections for CD31 expression. As shown in Supporting Fig. S2, the rim region proved to be more vascularized in comparison to the central portion of the tumor. In the latter zone, few vessels surrounded tumor cells and in some cases no vessels were detectable. These data underline that environment is a potent modulator of the phenotype and hence highlight the importance of an in-depth proteomic investigation.

Having defined these zones of interest, corresponding tissue material sampled from eight individual lesions (patients 1-8) was macrodissected and subjected to in-depth proteomic analysis. Normal tissue sampled at a distance (>5 cm) from the metastatic lesion (originating from the same patients) was also included in the proteomic analysis (here featuring the fourth zone). The rationale for including this fourth specimen was supported by imaging analysis of this tissue (Supporting Fig. S1a), where normal liver exhibited a distinct peptide distribution in comparison to other

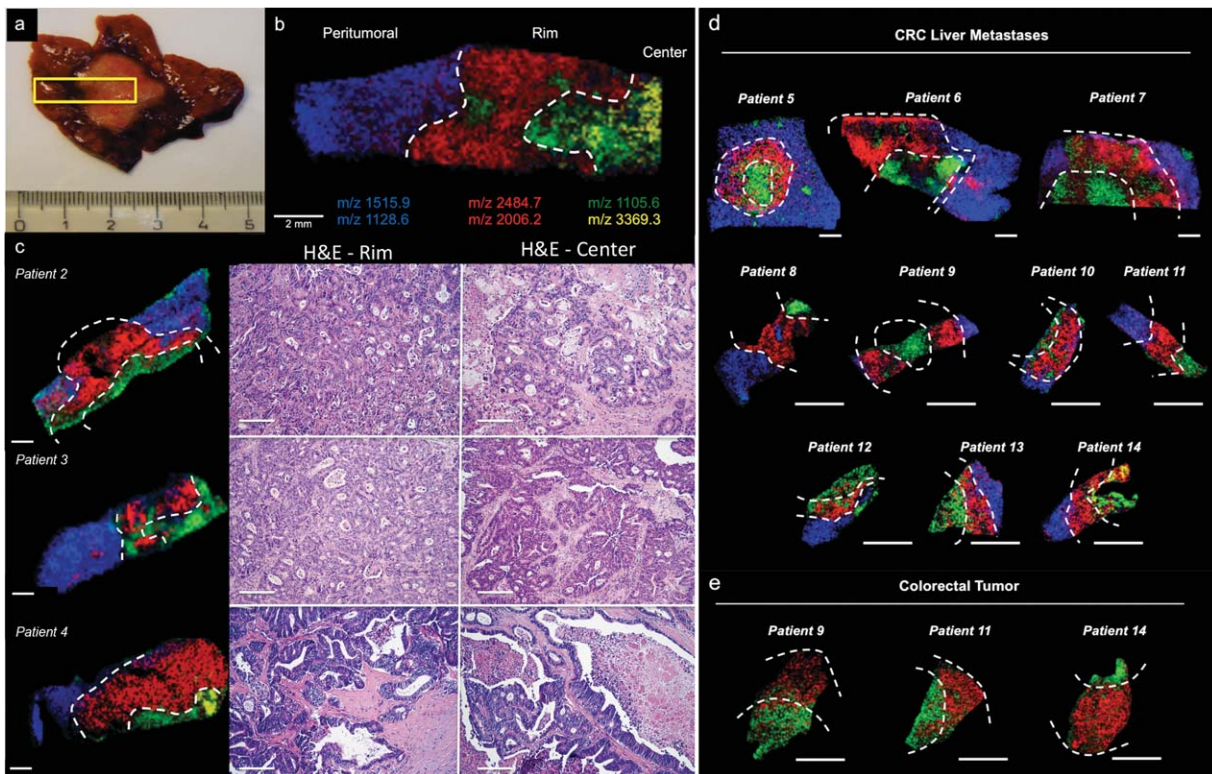


Fig. 1. Peptide MALDI-imaging of CRC liver metastases (14 cases) and primary colorectal tumors (3 cases). (A) Section of CRC liver metastasis containing the tumoral center, rim, and normal peritumoral tissue, with the area within the yellow rectangle analyzed in (B). (B) MALDI-imaging analysis of tryptic peptides within the sampled tissue section (patient 1, see Supporting Table S3). Three zones are distinguishable bearing unique peptide signatures (detailed in Supporting Fig. S1); the zones are divided with dashed lines indicating the macrodissected regions, which were sampled and latter subjected to MS analysis. Examples of representative peptides found in respective zones: (1) peritumoral zone 1515.9 m/z and 1128.6 m/z, rim 2484.7 m/z and 2006.2 m/z, and center 1105.6 m/z and 3369.3 m/z. Of the two peptides found in the central zone, 1105.6 m/z was present in all liver metastases analyzed, whereas peptide 3369.3 m/z was absent in some of the cases. (C) Three cases of CRC liver metastasis (patients 2-4) that were subjected to MALDI-imaging with representative hematoxylin/eosin (H&E) staining of rim and center of CRC liver metastasis (magnification 100 $\times$ ). (D) MALDI-imaging of 10 cases of CRC liver metastasis (patients 5-14) and (E) three primary colorectal carcinoma, which were obtained from patients 9, 11, and 14. (C-E) Color-coding corresponds to the peptides outlined in panel B. All scale bars are corresponding to 2mm, except (C) H&E staining is 100  $\mu$ m.

zones. We identified and quantified over 4,400 proteins, of which 1,067 were present in at least five out of eight individuals and were further considered in the present study. This selection was performed in order to highlight the most significant and robust candidates and discard those proteins that were variable between individuals and could represent false-positive hits. The selected proteins were further subjected to PCA (Fig. 2A) and Pearson correlation clustering (Fig. 2D) according to the respective protein abundance in each region. The analysis revealed that each individual zone contained a unique group of proteins defining its signature in addition to proteins that exhibited quantitative overexpression in some regions compared to other (Fig. 2B). The data show for the first time that peritumoral tissue, which is considered histologically normal, is proteomically and hence functionally distinct from normal tissue sampled far from the metastatic site.

The rim and the central region of the metastasis are particularly interesting for targeted therapy applications. Indeed, antibodies targeting biomarkers that are selectively expressed in these two zones bear the best chances to reach all malignant cells, which is an important prerequisite for optimal therapeutic outcome in clinics. Therefore, we have defined a region of interest (ROI) (Fig. 2A), within which most proteins cover the main part of the metastatic lesion (rim and center). All proteins further highlighted in this study are found within this ROI (also Supporting Table S1).

The PCA-derived protein clusters were further analyzed using the Ingenuity Pathways Analysis software. As displayed in Fig. 2C, distinct biological functions were associated to proteins overexpressed in particular regions, indicating that a specific pattern of functional heterogeneity exists within the CRC liver metastasis. Particularly significant is the finding that the

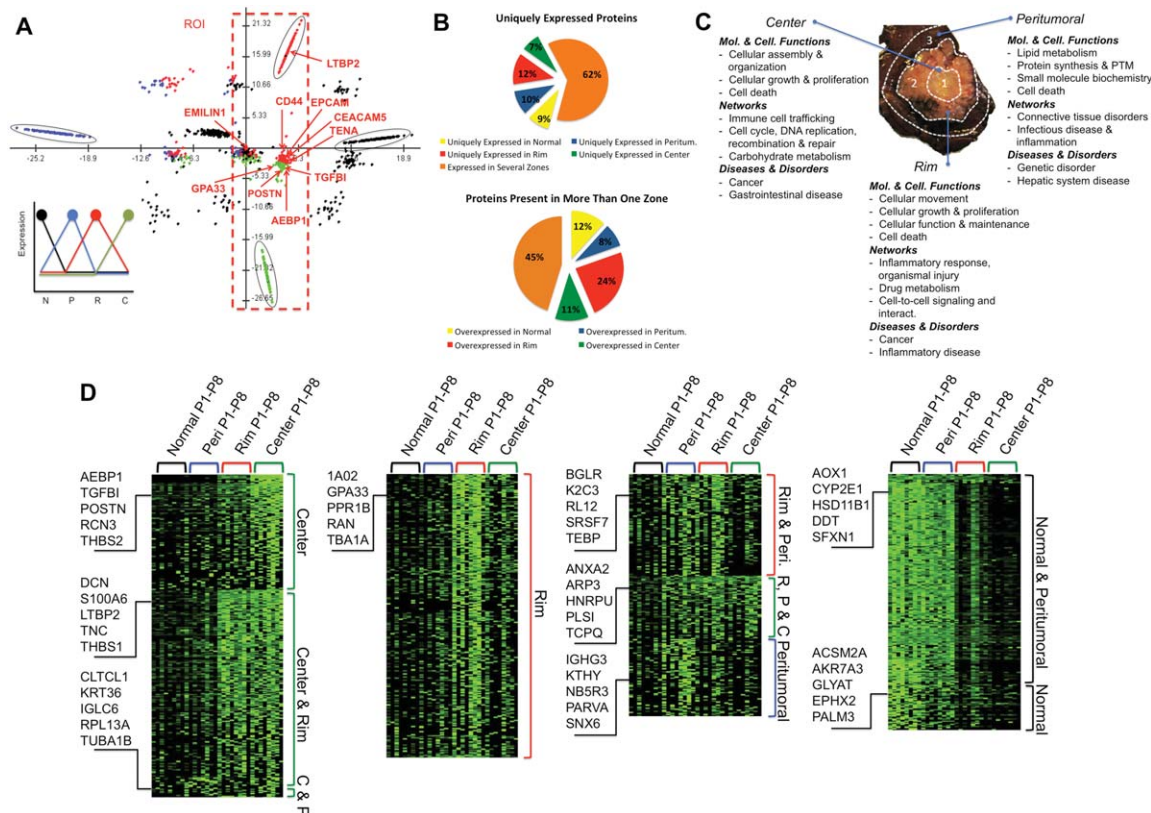


Fig. 2. Proteomic analysis of expression patterns within different zones of liver metastasis. (A) PCA of a representative CRC liver metastasis sample. Proteins show clustering according to their expression pattern and zone where they have been identified. Color-coding stands for proteins overexpressed in the normal (black), peritumoral (blue), rim (red), and center (green) zones. Proteins that are uniquely found in one of these respective zones are additionally encircled. An area of interest (ROI) was defined (dashed rectangle) to include the proteins of potential clinical value, showing increased expression in the rim and central region of the metastasis. All proteins investigated in the current study are found in this zone (these proteins are also displayed in Fig. 3). (B) Pie-chart featuring average percentages reflecting the number of proteins found uniquely (upper panel) or overexpressed (lower panel) in a particular regions of liver metastasis. (C) Ingenuity pathways analysis of clusters found in the PCA. The role of individual proteins was examined with respect to involvement in specific molecular and cellular functions, networks, diseases, and disorders. Top functions were highlighted. (C) Pearson correlation clustering of proteins that were expressed in at least five out of eight patients. Top five ranked proteins are highlighted. Color-coding corresponds to the level of protein expression (bright green signifies highest expression).

peritumoral region displayed a marked increase of lipid metabolism (cytochrome-c oxidase activity, catalysis of acyl-CoA from fatty acids and gluconeogenesis), protein synthesis, and posttranslational modifications (homotetramerization, proteolysis, and oxidation) as well as small molecule biochemistry (metabolism of hydrogen peroxide, protection against the peroxidation of lipids, and oxidation of NADH). The rim region is mainly characterized by the predominant expression of proteins taking part in cellular movement, proliferation, assembly, organization, and drug metabolism. The central region principally harbors proteins involved in cell death, inflammation, DNA-repair, and carbohydrate metabolism (detailed in the Supporting Table S2).

Next we performed Pearson correlation clustering of the 1,067 proteins identified in at least five out of

eight patients (Fig. 2D). The data confirmed the observations made in the PCA analysis and MALDI-imaging analysis, showing a zonally delineated pattern of expression. Figure 2D highlights the top five proteins that appeared in each cluster. Proteins of particular relevance for tumor targeting (having a potentially accessible nature and are expressed in the peritumoral, rim, and center of the metastasis) are further detailed in the Supporting Table S1.

**Known Protein Targets Show Distinct, Quantitative, Zonal Variations Within Liver Metastasis.** Starting from the defined ROI (Fig. 2A), we performed a comprehensive data-mining search for biomarkers already approved by the Food and Drug Administration (FDA) as therapeutic targets for solid tumors and among these some were found in the current study (Fig. 3A): cell surface A33 antigen (GPA33), epithelial

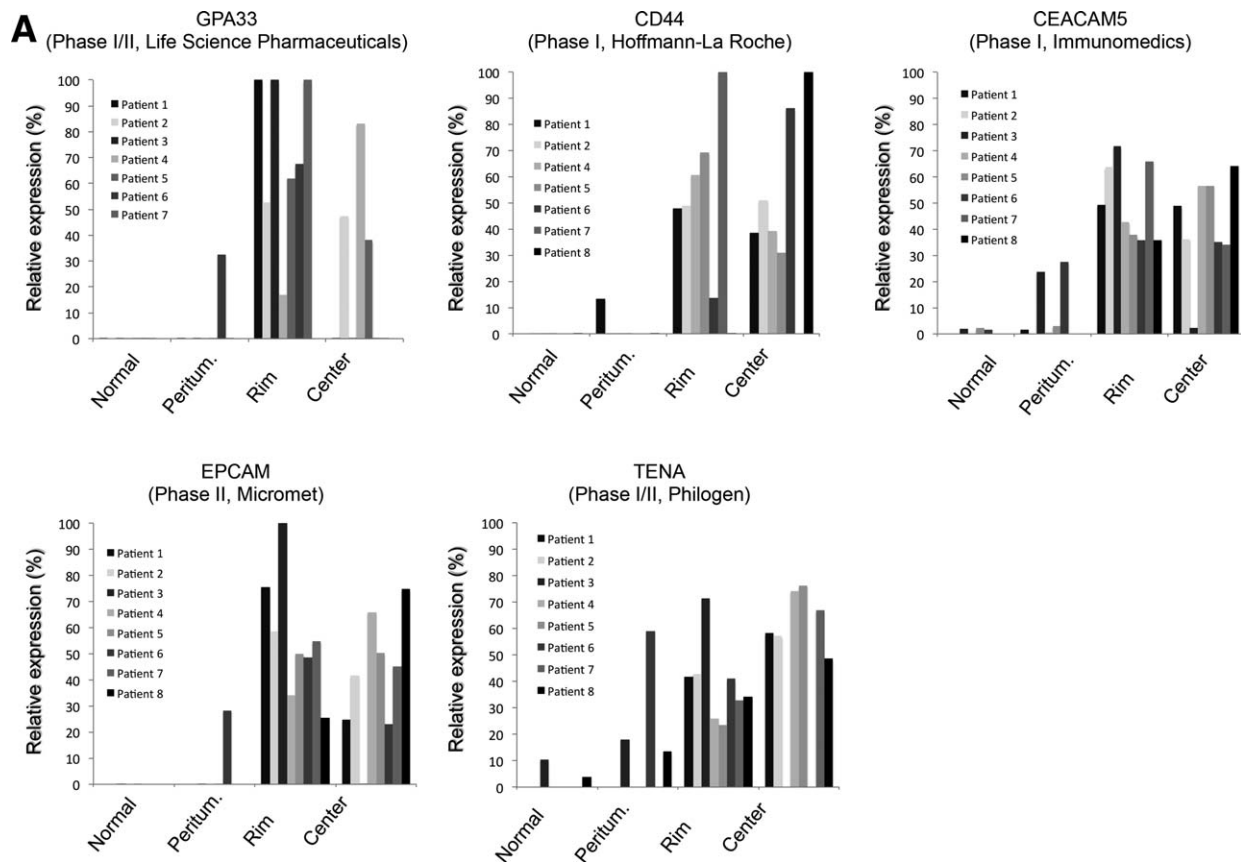


Fig. 3. Intratumoral distribution of known and novel protein antigens of value for targeted therapy applications. (A) MS quantitative protein analysis data on a set of known antigens already used in clinical trials for tumor therapy. Histograms indicate the quantification of relative protein expression of GPA33, EPCAM, TENA, CD44, and CEACAM5 per individual zone of liver metastasis in eight patients. Clinical trial phase and sponsor are indicted in brackets. (B) Novel antigens highlighted through present analysis and previously not identified in the context of CRC and liver metastasis. Histograms represent MS quantification of relative protein expression of AEBP1, EMILIN1, LTBP2, POSTN, and TGFBI per zone of liver metastasis derived from eight individual patients.

cell adhesion molecule (EPCAM), tenascin (TENA), CD44, and carcinoembryonic antigen-related cell adhesion molecule 5 (CEACAM5). Of these, A33 and CEACAM5 trials include CRC liver metastasis cases. GPA33, CD44, and EPCAM were found expressed both in the rim and the central region of the metastasis; however, up to 9-fold more concentrated in the center. CEACAM5 was also found expressed in the rim and the central region but displayed no significant difference between the two. TENA was detected in all four regions, ranging from low expression in the normal and peritumoral region to high expression in the rim and central zone of the metastasis, with a clear tendency of 2-fold overexpression in the center in comparison to the rim.

Because of their unique ability to divide indefinitely, cancer stem cells are identified as key therapeutic targets by an increasing number of studies.<sup>16-19</sup> We analyzed the acquired proteomic data and assessed the spatial distribution of accessible proteins frequently

encountered in cancer stem cells (Supporting Fig. S3). Of the highlighted proteins, CD133, CD90, and ANXA3 show prominent expression in both the rim and central region and therefore appear particularly appealing for considering them in the context of targeted therapy.

**Novel Accessible Proteins With Potential Value for Targeted Therapy of Liver Metastases.** Owing to the particular analytical approach, in the current study we identified a panel of proteins that have the potential to become target molecules for therapeutic applications (detailed in the Supporting Table S1). Pearson correlation clustering (see top five candidates in Fig. 2D) has highlighted proteins that were particularly relevant, because they have been found tightly associated with a particular pattern of expression and were present in the greatest number of individuals examined. Of the highlighted proteins, several candidates have previously been found in similar proteomic studies of primary breast,<sup>14</sup> colon,<sup>20</sup> and pancreas<sup>13</sup> carcinomas, pointing

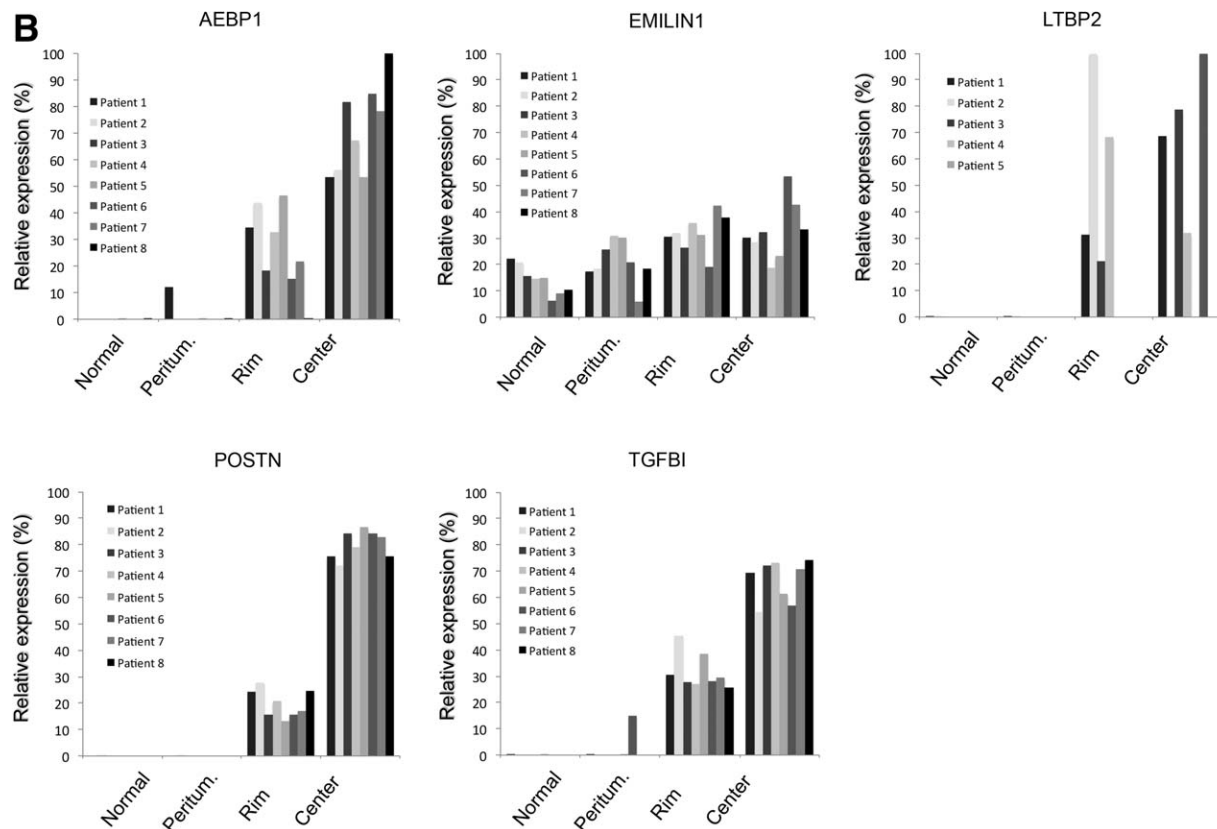


Fig. 3. Continued.

at their apparent characteristic of being intimately associated with the tumorigenic process. In the current work we therefore choose to particularly highlight these proteins: adipocyte enhancer-binding protein 1 (AEBP1), elastin microfibril interface-located protein 1 (EMILIN1), latent-transforming growth factor beta-binding protein 2 (LTBP2), periostin (POSTN), and transforming growth factor-beta-induced protein ig-h3 (TGFBI) (Fig. 3B). Of these, only EMILIN1 showed expression in all zones examined, with the highest concentration detected in the rim. The remaining proteins were found in the rim and central region of the metastasis, with LTBP2 mainly detected in the rim and the AEBP1, POSTN, and TGFBI in the central region of the tumor. In order to verify their differential zonal expression, the antigens, were further tested using IHC analysis in 19 additional cases of CRC liver metastases (Fig. 4). Evaluation of the staining pattern revealed that all five antigens were predominately accumulated in an area rich in tumor desmoplastic reaction. Tumor cells were predominately negative when stained for AEBP2, EMILIN1, and POSTN, but were positive for LTBP2 and TGFBI. In normal human tissues, these proteins are mainly absent or have low detection levels (detailed in the Supporting Materials).

**Correlation Analysis With High-Throughput Genomic Studies Identifies Common Targets.** We compared several genetic studies that have either profiled CRC liver metastases or examined primary metastatic and nonmetastatic CRC. Owing to the comparative analysis with datasets from five different genetic studies,<sup>21-25</sup> we found 131 proteins that were in common with our present study. The data are further outlined in the Supporting Materials and Fig. S7.

**TGFBI and LTBP2 Are Widely Expressed in Human Liver Metastases and Can Be Targeted In Vivo.** Liver lesions originating from four patients (patients 4-7, who were also involved in MS analysis) were macrodissected according to the previously established zones and subjected to WB analysis (Fig. 5A). The results showed that both TGFBI and LTBP2 are detected in all the lesions analyzed. In accordance with the MS data (Fig. 3B), the two antigens displayed a different intratumoral distribution. TGFBI generally accumulated more in the center, whereas LTBP2 was predominantly found in the rim region. In patient 4, the trend was inverted, suggesting a possible interindividual variation. The presence of TGFBI and LTBP2 was further confirmed in seven

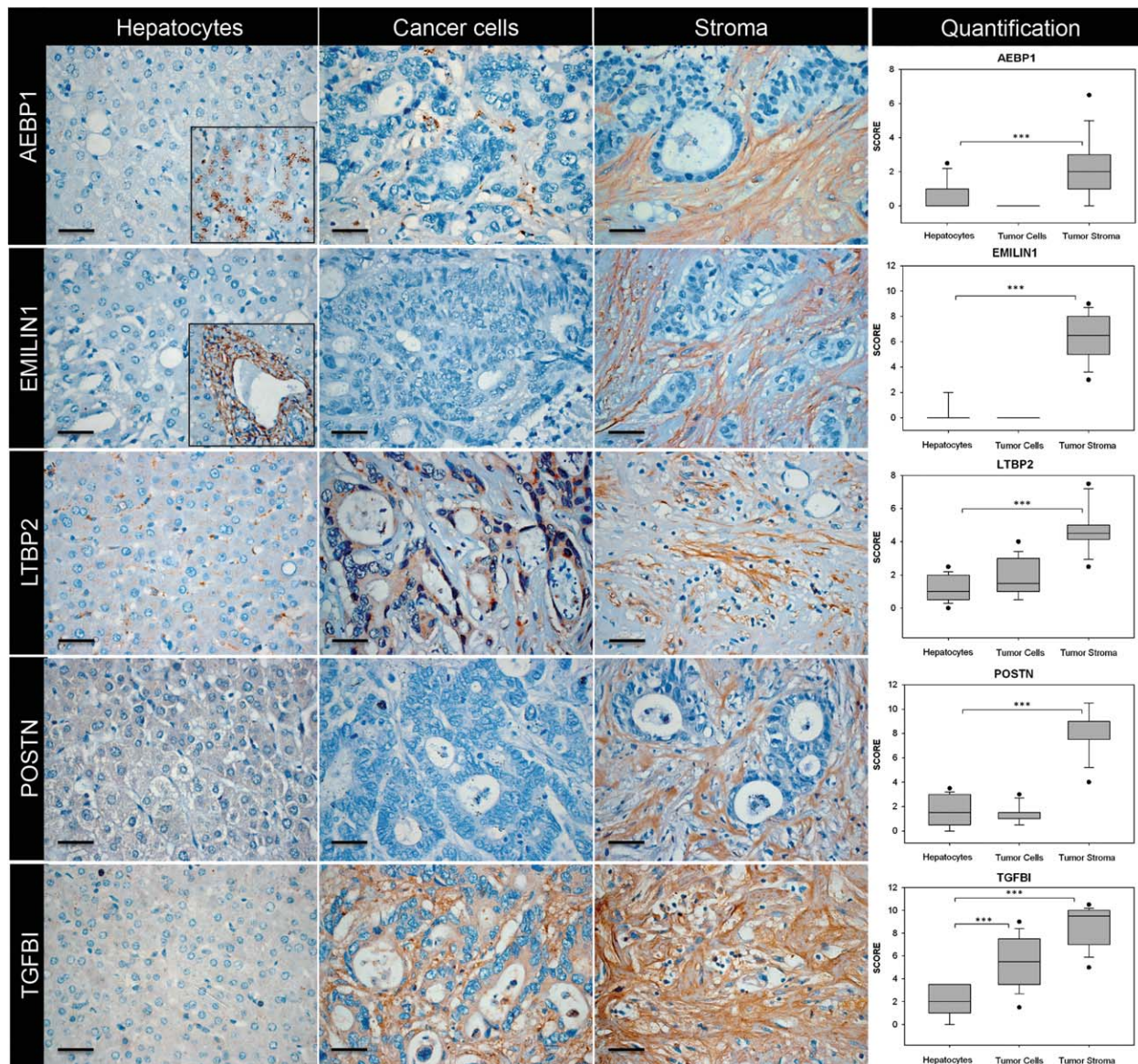


Fig. 4. Immunohistochemical analysis of novel proteins overexpressed in CRC liver metastasis. Nineteen individual cases (patients 15-33, see Supporting Materials) were examined and one representative image is shown in the current figure. Displayed are expression patterns of AEBP1, EMILIN1, LTBP2, POSTN and TGFB1, assessed in (1) normal adjacent tissue, (2) cancer cells in the liver metastasis, and (3) stromal tissue, both found within the liver metastasis lesion. AEBP1 and EMILIN1 normal tissue panels feature boxes where some positive cells are displayed. These were few in number yet present and confirmed not to be hemosiderin artifacts, often found in IHC performed with liver samples. Magnification 400 $\times$  and the scale bars are corresponding to 20  $\mu$ m. Semiquantitative evaluation of IHC staining was performed as outlined in the Experimental Procedures (Supporting Materials).

additional CRC liver metastasis cases (Fig. 5A, patients 8-14), with an evident trend of overexpression for both biomarkers in the metastatic lesion (except patient 12, where only low TGFB1 levels were detected). We further sought to test whether LTBP2 and TGFB1 are expressed in liver metastases originating from other primary tumors. As shown in Fig. 5B, both biomarkers were detected in liver metastases originating from lung, pancreas, or breast

primary tumors. In order to test the specificity of both antigens, their expression was evaluated in a series of liver cirrhosis cases of toxicological and viral origin (Fig. 5C). This was important in order to exclude the possibility that these antigens are expressed due to inflammation, which is an important constituent of cancer. Both antigens showed no reactivity in cirrhosis tissues, suggesting that their expression in CRC liver metastases is not due to



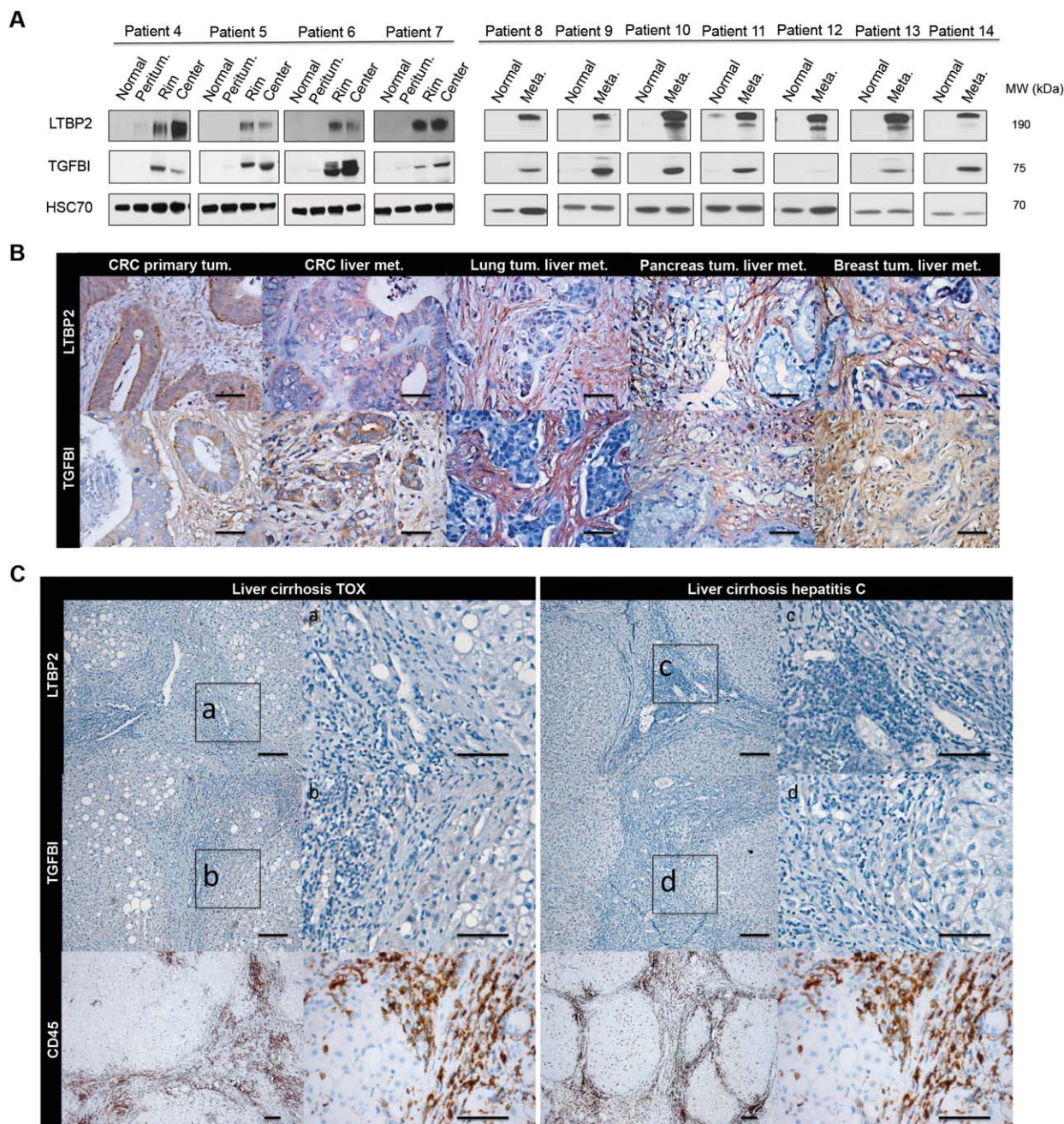


Fig. 5. Western blot validation of LTBP2 and TGFBI protein expression in tissues from 11 additional CRC liver metastasis patients. (A) Four CRC liver metastases were macrodissected in different zones and used to further validate protein expression of the two protein targets. Seven further cases of CRC liver metastasis were also assessed for the expression of LTBP2 and TGFBI proteins. Molecular weight scale depicts the observed protein weight following sodium dodecyl sulfate-polyacrylamide gel electrophoresis-based protein separation (SDS-PAGE). HSC70 protein was used for normalization purposes. (B) IHC evaluation of LTBP2 and TGFBI protein expression in primary colorectal tumors as well as liver metastases from colorectal, lung, pancreas, and breast primary tumors. Displayed are representative images of at least five individual cases (for CRC 15 cases) for each disease category. Magnification 400 $\times$ , scale bars 20  $\mu$ m. (C) (upper and middle panel) IHC analysis of LTBP2 and TGFBI protein expression in liver cirrhosis as a common inflammatory liver disease. Ten individual cases of alcohol (TOX) or viral (hepatitis C) promoted liver cirrhosis were evaluated (one representative case is shown per condition). Magnification of 100 $\times$  was used; scale bars correspond to 50  $\mu$ m. Highlighted areas (a-d) (marked with the black squares) are shown at 400 $\times$  magnification. (lower panel) CD45 staining confirms the presence of inflammatory cells (magnification 50 $\times$  and 400 $\times$ ; scale bars denote 50  $\mu$ m).

inflammatory reaction. Finally, we tested if antibody-based tumor targeting of TGFBI and LTBP2 is feasible *in vivo*. The results show that both proteins are

accessible and reachable for fluorescently labeled intravenous injected homing antibodies (further outlined in the Supporting Materials).

## Discussion

The ever-increasing appreciation of tumor heterogeneity at the individual and intratumoral levels has clearly identified this as a major hurdle for the development of successful targeted anticancer treatments. Future effective therapeutic strategies will inevitably depend on the ability to further characterize and take into account tumor heterogeneity. We contribute to this effort by characterizing for the first time the proteomic heterogeneity of human liver metastases through a relevant example of liver-disseminated CRC. The proteomic approach was important because extrapolations from existing genomic studies<sup>4-6</sup> could lead to the prediction that cancer lesions are stochastically heterogeneous at the protein level too. The data outlined here indicate that this is not the case, and suggest that the tumor microenvironment in CRC liver metastases forces a more general phenotype despite the genetic status of individual cancer cells. We show that this is particularly true for vascularization in the CRC liver metastases, which certainly imposes variations in oxygen tension and nutrient availability.

The present data have expectedly shown the unlikely existence of a “super” target that will alone homogeneously cover the entire tumor lesion. Our study unexpectedly demonstrated that the heterogeneity in CRC liver metastasis at the protein level displays a consistent and organized pattern, offering an alternative route to approach the problem of failing targeted therapies in a structured fashion. Namely, based on this proteomic characterization of individual zones within the CRC liver metastasis, it is possible to select a set of antigens that would in combination homogeneously target the entire lesion. In line with this view, we characterized biomarkers relevant for such therapeutic approaches and examined known and novel candidates for their intrametastatic distribution. Of the known protein targets, TENA seem promising for treating CRC liver metastasis, as this protein covers both the tumoral and the peritumoral regions. Other particularly relevant biomarkers for antibody-based targeted therapies are EPCAM and CD44. These proteins show a favorable distribution with respect to absence in normal liver tissue and accumulation in the center and rim of the metastasis as well as being a reported marker of CRC stem cells. However, CD44 and EPCAM are shared between cancer stem and liver progenitor cells, and therefore their targeting might also destroy the latter cell subpopulation, which is particularly important for liver

regeneration following injury/disease. Concerning the novel targets, LTBP2 and TGFBI seem particularly suitable for liver metastasis targeted therapy. Both antigens show high expression in numerous cases of liver metastasis of different primary origin and are concentrated both in the stroma and tumor cells. Importantly, they are generally neither expressed in normal tissues nor in noncancerous inflammatory liver lesions (such as viral and alcohol-caused cirrhosis). Although recent data<sup>26-29</sup> provide evidence that TGFBI and LTBP2 are relevant actors in cancer, their functional aspects remain to date elusive and contradictory.<sup>27,28</sup> The current study has not attempted to clarify this question because we considered these proteins not as functional targets. Their increased, specific presence in cancer lesions is certainly a criterion good enough to use them as anchor points for delivery of antibody-drug conjugates (ADC). We therefore used a chicken-chorioallantoic membrane-based CRC *in vivo* model to demonstrate that both LTBP2 and TGFBI can be reached by way of intravenous injection of homing antibodies, used in the present case to deliver fluorescent agent (Supporting Data). The next step would inevitably involve similar testing on mouse orthotropic models. Our preliminary data show that in the mouse model (which would probably be the case in human as well) targeting liver metastasis requires smaller antibodies, lacking Fc regions, because full format IgG are easily trapped in the normal liver (probably through Fc receptors on Kupffer cells). Similarly, this is readily observed with radiolabeled Cetuximab<sup>30</sup> (anti-EGFR), indicating the limitation of IgG format antibodies, especially to serve as ADC. Therefore, future work should include the generation of smaller antibody fragments for TGFBI and LTBP2 for murine biodistribution studies. These data will permit the final assessment of the usefulness of these two proteins to serve as therapeutic targets for an ADC approach.

*Acknowledgment:* The authors thank the GIGA-proteomics platform (University of Liège [ULG]) for mass spectrometry analysis, BIOBANK (ULG) for tissue material as well as Pascale Heneaux and Evgenia Turtoi for experimental support. The authors thank Dr. Mark E. Sobel for proofreading the article.

## References

1. Garattini L, van de Vooren K, Zaniboni A. Ethics for end-of-life treatments: metastatic colorectal cancer is one example. *Health Policy* 2012; 109:97-103.

2. Gillies RJ, Verduzco D, Gatenby RA. Evolutionary dynamics of carcinogenesis and why targeted therapy does not work. *Nat Rev Cancer* 2012;12:487-493.
3. Diaz LA Jr, Williams RT, Wu J, Kinde I, Hecht JR, Berlin J, et al. The molecular evolution of acquired resistance to targeted EGFR blockade in colorectal cancers. *Nature* 2012;486:537-540.
4. Navin N, Kendall J, Troge J, Andrews P, Rodgers L, et al. Tumour evolution inferred by single-cell sequencing. *Nature* 2011;472:90-94.
5. Yachida S, Jones S, Bozic I, Antal T, Leary R, Fu B, et al. Distant metastasis occurs late during the genetic evolution of pancreatic cancer. *Nature* 2010;467:1114-1117.
6. Gerlinger M, Rowan AJ, Horswell S, Larkin J, Endesfelder D, Gronroos E, et al. Intratumor heterogeneity and branched evolution revealed by multiregion sequencing. *N Engl J Med* 2012;366:883-892.
7. Ferlay J, Shin HR, Bray F, Forman D, Mathers C, Parkin DM. Estimates of worldwide burden of cancer in 2008: GLOBOCAN 2008. *Int J Cancer* 2010;127:2893-2917.
8. Kopetz S, Chang GJ, Overman MJ, Eng C, Sargent DJ, Larson DW, et al. Improved survival in metastatic colorectal cancer is associated with adoption of hepatic resection and improved chemotherapy. *J Clin Oncol* 2009;27:3677-3683.
9. Hoyer M, Swaminath A, Bydder S, Lock M, Mendez Romero A, Kavanagh B, et al. Radiotherapy for liver metastases: a review of evidence. *Int J Radiat Oncol Biol Phys* 2012;82:1047-1057.
10. Caprioli RM, Farmer TB, Gile J. Molecular imaging of biological samples: localization of peptides and proteins using MALDI-TOF MS. *Anal Chem* 1997;69:4751-4760.
11. Kang S, Kim MJ, An H, Kim BG, Choi YP, Kang KS, et al. Proteomic molecular portrait of interface zone in breast cancer. *J Proteome Res* 2009;9:5638-5646.
12. Kang S, Shim HS, Lee JS, Kim DS, Kim HY, Hong SH, et al. Molecular proteomics imaging of tumor interfaces by mass spectrometry. *J Proteome Res* 2010;9:1157-1164.
13. Turtoi A, Musmeci D, Wang Y, Dumont B, Somja J, Bevilacqua G, et al. Identification of novel accessible proteins bearing diagnostic and therapeutic potential in human pancreatic ductal adenocarcinoma. *J Proteome Res* 2011;10:4302-4013.
14. Turtoi A, Dumont B, Greffe Y, Blomme A, Mazzucchelli G, Delvenne P, et al. Novel comprehensive approach for accessible biomarker identification and absolute quantification from precious tissues. *J Proteome Res* 2011;10:3160-3182.
15. Saeed AI, Bhagabati NK, Braisted JC, Liang W, Sharov V, Howe EA, et al. TM4 microarray software suite. *Method Enzymol* 2006;411:134-193.
16. McCubrey JA, Steelman LS, Abrams SL, Misaghian N, Chappell WH, Basecke J, et al. Targeting the cancer initiating cell: the ultimate target for cancer therapy. *Curr Pharm Des* 2012;18:1784-1795.
17. Harris PJ, Speranza G, Dansky Ullmann C. Targeting embryonic signaling pathways in cancer therapy. *Expert Opin Ther Targets* 2012;16:131-145.
18. Binello E, Germano IM. Stem cells as therapeutic vehicles for the treatment of high-grade gliomas. *Neuro Oncol* 2012;14:256-265.
19. Ping YF, Bian XW. Concise review: contribution of cancer stem cells to neovascularization. *Stem Cells* 2011;29:888-894.
20. Conrotto P, Roesli C, Rybak J, Kischel P, Waltregny D, Neri D, et al. Identification of new accessible tumor antigens in human colon cancer by ex vivo protein biotinylation and comparative mass spectrometry analysis. *Int J Cancer* 2008;123:2856-2864.
21. Pantaleo MA, Astolfi A, Nannini M, Paterini P, Piazzi G, Ercolani G, et al. Gene expression profiling of liver metastases from colorectal cancer as potential basis for treatment choice. *Br J Cancer* 2008;99:1729-1734.
22. Bertucci F, Salas S, Eysteris S, Nasser V, Finetti P, Ginestier C, et al. Gene expression profiling of colon cancer by DNA microarrays and correlation with histoclinical parameters. *Oncogene* 2004;23:1377-1391.
23. Fritzmann J, Morkel M, Besser D, Budczies J, Kosel F, Brembeck FH, et al. A colorectal cancer expression profile that includes transforming growth factor beta inhibitor BAMBI predicts metastatic potential. *Gastroenterology* 2009;137:165-175.
24. Lin AY, Chua MS, Choi YL, Yeh W, Kim YH, Azzi R, et al. Comparative profiling of primary colorectal carcinomas and liver metastases identifies LEF1 as a prognostic biomarker. *PLoS One* 2011;6:e16636.
25. Sun L, Hu H, Peng L, Zhou Z, Zhao X, Pan J, et al. P-cadherin promotes liver metastasis and is associated with poor prognosis in colon cancer. *Am J Pathol* 2011;179:380-390.
26. Ween MP, Oehler MK, Ricciardelli C. Transforming growth factor-beta-induced protein (TGFBI)/( $\beta$ ig-H3): a matrix protein with dual functions in ovarian cancer. *Int J Mol Sci* 2012;13:10461-10477.
27. Zhang Y, Wen G, Shao G, Wang C, Lin C, Fang H, et al. TGFBI deficiency predisposes mice to spontaneous tumor development. *Cancer Res* 2009;69:37-44.
28. Ma C, Rong Y, Radloff DR, Datto MB, Centeno B, Bao S, et al. Extracellular matrix protein betaig-h3/TGFBI promotes metastasis of colon cancer by enhancing cell extravasation. *Genes Dev* 2008;22:308-321.
29. Chan SH, Yee Ko JM, Chan KW, Chan YP, Tao Q, Hyytiainen M, et al. The ECM protein LTBP-2 is a suppressor of esophageal squamous cell carcinoma tumor formation but higher tumor expression associates with poor patient outcome. *Int J Cancer* 2011;129:565-573.
30. Aerts HJ, Dubois L, Perk L, Vermaelen P, van Dongen GA, Wouters BG, Lambin P. Disparity between in vivo EGFR expression and 89Zr-labeled cetuximab uptake assessed with PET. *J Nucl Med* 2009;50:123-131.